CORROSION SCIENCE AND TECHNOLOGY, Vol.31, No.2(2002), pp.149~155

A Study on the Flow-Accelerated Corrosion Characteristics of Galvanically Coupled Dissimilar Metals

YoonSeok Choi and JungGu Kim

Department of Advanced Materials Engineering, Sung Kyun Kwan University
300 Chunchun-Dong, Jangan-Gu, Suwon 440-746, KOREA

The flow-accelerated corrosion characteristics of a carbon steel(CS) coupled to stainless steel(SS) were investigated in deaerated alkaline-chloride solutions with velocities (0, 0.2, 0.4 and 0.6 m/s), pH (8, 9 and 10) and temperatures (25, 50 and 75℃). The electrochemical properties of specimens were investigated by potentiodynamic test and galvanic corrosion test using RCE (Rotating Cylinder Electrode). CS did not show passive behavior while SS show passive behavior in the alkaline-chloride solution. Galvanic corrosion tests were conducted as a function of flow velocities, pH and temperature. The galvanic current density increases with increasing flow velocity and temperature, but decreased with increasing pH. Flow velocity had a small effect on the galvanic current density at 25℃, whereas the flow velocity increased galvanic current density significantly at 50 and 75℃. This might be due to the increased solubility of magnetite at the higher temperature.

Keywords : *Flow-accelerated corrosion, galvanic corrosion, flow effect, pH, temperature, carbon steel, stainless steel, magnetite*

1. Introduction

Corrosion and electrochemical materials wastage processes take on many different forms.[1] Most of these forms are dramatically affected by the relative flow rates of the reactants in the corroding cell. It is well known that relative electrolyte velocity can strongly influence rates and mechanisms of corrosion.[2] One of most important factors affecting corrosion reactions in the presence of a flowing liquid is the linear velocity of the flowing fluid at the interface of the metal or metal oxide surface and the flowing fluid. This linear velocity is not, of necessity, equal to the bulk flow rate. Another important factor is the turbulence which occurs at the interface of the metal oxide surface and the flowing fluid.

Two wide areas of flow-dependant corrosion have been distinguished[3]; namely, corrosion due to mass transfer and corrosion influenced by mechanical flow effects. These types of corrosion are described according to their appearances and causes, which are brought about by the flow mechanics of the system. In corrosion due to mass transfer, corrosion is caused mainly by the transport of reactants and reaction products but not by shear stress or other mechanical influences. The flow-dependency of the corrosion system is greater or smaller according to whether it is predominantly materials-transport controlled or reaction controlled. Flow-accelerated corrosion (FAC) may be defined as the result of a material loss that occurs through the alternate dissolving of the normally protective oxide layer that typically forms on the surface of many materials, followed by the reformation of the protective layer.[4] One unusual and identifying characteristic of FAC of low carbon steel is that the magnetite (Fe_3O_4) layer, normally protective iron oxide, is chemically dissolved by the flowing water stream.[5]

The galvanic cells established by dissimilar metals in the water were major cause of corrosion failures.[6] Deposits on the anodic surfaces normally of higher resistance than bare metal tended to lower the corrosion rate. However, where these deposits were dissolved by the flowing water stream, the corrosion reaction continued.

In this work, the effect of galvanic corrosion on the FAC with different flow velocity, pH and temperature was studied using electrochemical measurements with a rotating cylinder electrode.

2. Experimental

2.1 Materials and preparation

Carbon steel (AISI 1010: CS) and stainless steel (AISI 304: SS), with the chemical composition shown in Table 1,

Table 1. Chemical compositions of specimens(%)

	C	Al	Mn	P	S	Si	Cr	Ni	Fe
AISI1010	0.12	0.03	0.43	0.018	0.014	0.21	-	-	bal.
AISI304	0.08	-	2.0	0.045	0.03	1.0	18	8	bal.

were used in the present study. The geometry of a specimen was cylinder type of 1.3㎝ in diameter and 1.3㎝ in height. The outer surface of the cylinder was exposed in solution. The test surfaces were degreased with ethanol after being polished with #600 SiC paper.

2.2 Electrolytes

The deaerated alkaline-chloride solutions were used. Two factors were considered, pH (8, 9, 10) and temperature (25, 50, 90℃). For the purpose of acceleration, 200ppm of chloride was added. All solutions were deaerated with pure N2 at a flow rate of 10cc/min.

2.3 Potentiodynamic tests

To simulate fluid flow in pipes and tubes and to clarify the corrosion mechanism in the flow field, a rotating electrode is used often. In the laminar region, a rotating disk electrode (RDE) is applied to determine the rate-controlling process of the chemical or electrochemical reaction. In the turbulent flow region, a rotating cylinder electrode (RCE) can be applied to simulate flow behavior.[7]

In the present study, the RCE method was selected to simulate the flow field. The RCE has the characteristics of a uniform of current distribution and velocity profile in the axial direction with clearly defined hydrodynamics.[8,9] A PINE model AFMSRX analytical rotator was used to rotate the electrode. The velocity of the electrode was calculated using the formula:

$$V = \omega r$$

Where ω represents the angular velocity in radians/second and r is the radius of the electrode in meters. Flow rates 0, 0.2, 0.4 and 0.6 m/s were examined using this apparatus.

Electrochemical polarization of the sample was accomplished with an EG & G Model 273A potentiostat. The potentiostat was programmed to apply a continuously varying potential to the sample at a rate of 600 mV / h. The electrochemical test cell contained the working electrode, a glass capillary probe connected to a reference electrode, and two graphite rod counter electrode. All potentials were measured against the saturated calomel electrode (SCE). For each material and electrolyte combination, the corrosion sample was allowed to stabilize in the electrolyte, until the potential change was < 1mV/min. This potential then was taken as the open-circuit potential (OCP).

2.4 Galvanic corrosion tests

The nature and properties of the corrosion products that form on some metals or alloys are very important from the standpoint of resistance to FAC with fluid flow.[10] Thus, in the present study, the potentiostatic tests were performed at 200㎷$_{SCE}$ for 20 minutes to form the corrosion products at the CS(anode), before the galvanic corrosion tests.

For galvanic current measurements as a function of velocity, an electrode holder has been constructed which contains 2 dissimilar metals as shown in Figure 1.[11]

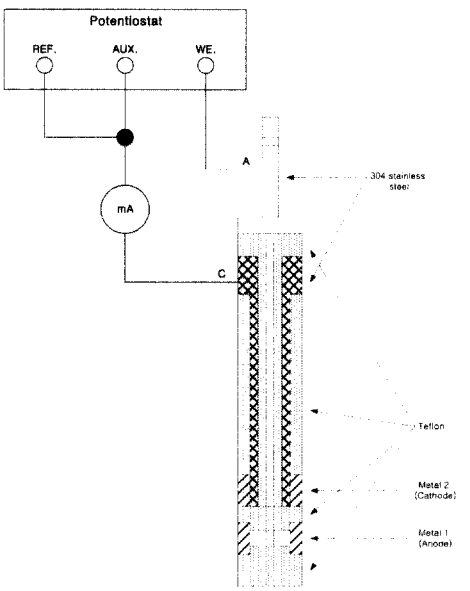

Fig. 1. Experimental arrangement for measurement of galvanic currents as a function of rotation speed.

The two dissimilar metal cylinders are connected to two metal shafts which are isolated from each other. Only the cylinder walls are contact with the electrolyte, a design which avoids edge effects. To evaluate the quantitative galvanic effect between CS and SS, galvanic corrosion tests were performed using a zero resistance ammeter. The CS is connected to the working electrode terminal (anode), the SS to the reference electrode terminal (cathode) which is connected to the counter electrode terminal.

The galvanic current and potential measured for 30 minutes at stagnant conditions. The rotation speed was then set to 0.2 m/s for 30 minutes and further increased to 0.4 and 0.6 m/s.[12] The ratio of the anode to the cathode for each test was 1 : 1.

2.5 Surface observations

Corrosion products on the metal surface were examined by scanning electron microscopy (SEM) and x-ray diffractometry (XRD).

3. Results and discussion

Figure 2 illustrates the anodic polarization curves of CS and SS as function of velocities (pH=8). CS exhibited active corrosion behavior, i.e., no passivation, and corrosion current density increased with increasing velocity. However SS showed passive behavior at all velocities and passive current density decreased with increasing flow velocity. These are due to the fact that the rate of reduction of water increased as increasing velocity. When the rate of cathodic reduction is sufficiently high, the anodic dissolution is accelerated by increasing flow velocity. Since CS exhibited active corrosion behavior, the corrosion rate rises to high value. On the other hand, in the case of SS, the passive state is stable, and passive current density falls to low values as increasing flow velocity.[13]

Figure 3 compares the corrosion potential between CS and SS as a function of velocity. The corrosion potential of CS and SS shift in the noble direction with increasing solution velocity.

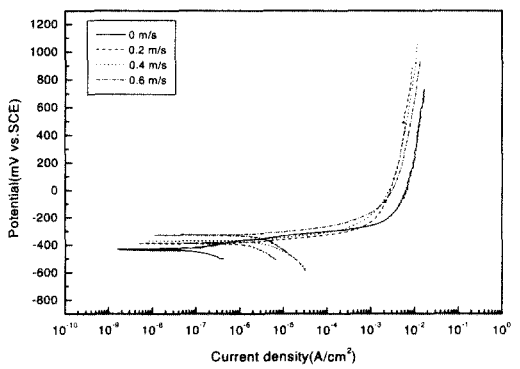

(a)

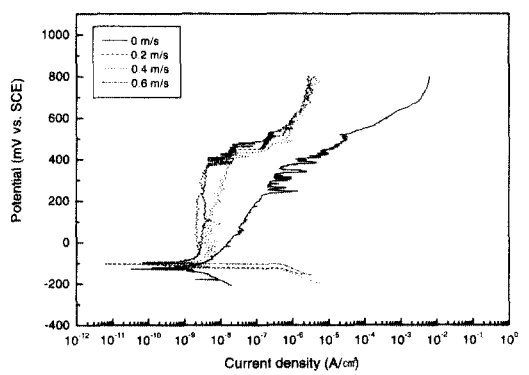

(b)

Fig. 2. Anodic polarization curves at different flow velocities(pH=8): (a) CS and (b) SS.

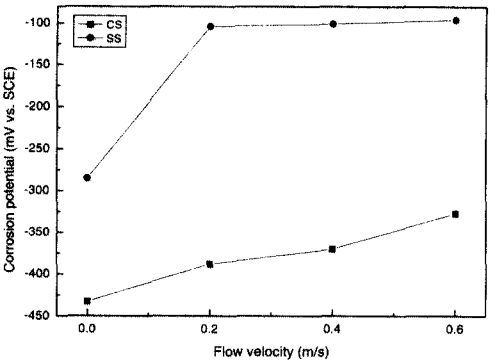

Fig. 3. Comparison of corrosion potential between CS and SS (pH=8).

These results suggest that the cathodic reaction that supports anodic polarization is diffusion controlled.[13] Uhlig and Revie[14] have suggested that only water is required to the anodic reaction of metal in a deaerated solution.

$$M + nH_2O \rightarrow MO(\text{passive film}) + nH^+ + ne^-$$

The cathodic reaction in a deaerated solution can be assumed to be the hydrogen reaction;

$$2H_2O + 2e^- \rightarrow H_2(gas) + 2OH^-(pH \geq 7)$$

From a kinetic point of view, it is unlikely that diffusion of water molecules to the alloy surface is rate controlling. Rather, it appears that desorption of clusters of hydrogen molecules is rate controlling and is enhanced by increasing flow rates. Thus, increasing electrode surface velocities and corresponding increases in flow rates effectively shift the corrosion potential in the noble direction.

The difference of corrosion potential between CS and SS becomes the driving force for galvanic corrosion. In Figure 3, the CS had a low corrosion potential than SS and the potential difference between CS and SS at a fixed velocity, increased with increasing flow velocity. This indicated that the CS acts as an anode when galvanically coupled, and the presence of fluid flow will be accelerated a galvanic effect.

3.1 Effect of flow velocity

Figure 4 shows the galvanic current density and galvanic potential of pre-charged and just immersion conditions recorded at the end of the 30 minute period at each rotation speed. For both conditions, the galvanic current density and potential increased with increasing velocity.

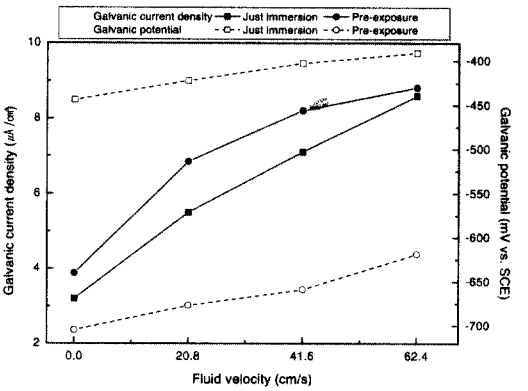

Fig. 4. Galvanic current density and potential as a function of velocity under just immersion and pre-exposure conditions

At pre-charged condition, however, higher current density and lower potential were measured than at the just immersion condition.

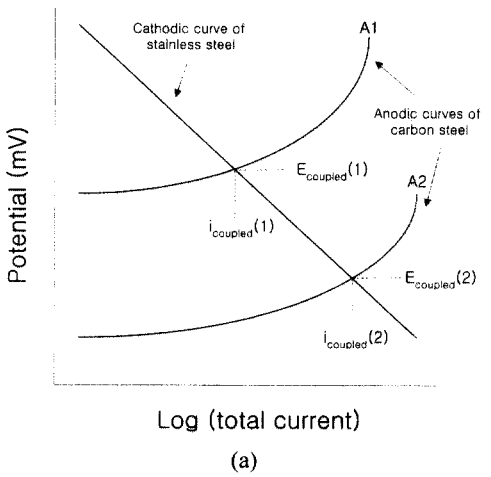

(a)

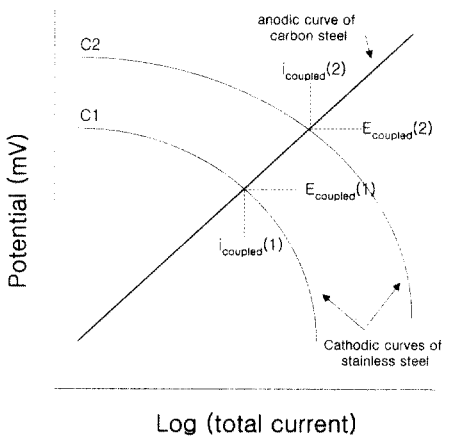

(b)

Fig. 5. Analysis of applied anodic potential and flow velocity effects.

This behavior was explained in Figure 5 (a). When anodic potential was applied, anodic curve of CS changed from A1 to A2, which shifted the galvanic current density and potential. Also, at each step-function increase in the velocity of the electrode, an instantaneous step-function increase in the galvanic current density is observed, indicating that the effect of increasing flow velocity is to increase the rate of the cathodic reduction reaction. Thus, the variation of galvanic current density and potential with flow velocity could be controlled by cathodic reaction (C1 →C2, Figure 5(b)).

3.2 Effect of pH

Figure 6 shows the galvanic current density and galvanic potential as a function of velocity at different pH. The galvanic current density decreased and potential increased with increasing pH. In Potential-pH diagram of Fe,[15] more stable magnetite (Fe_3O_4) form on surface of CS as increasing pH. Therefore, this stable oxide can be reduced galvanic corrosion between CS and SS.

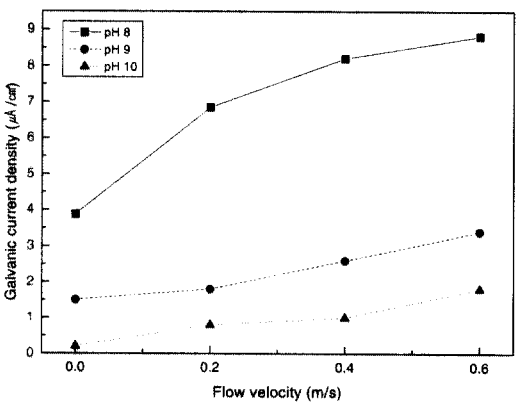

(a) Current density

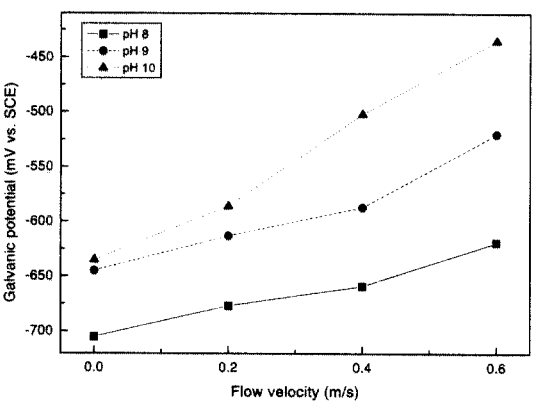

(b) Potential

Fig. 6. Galvanic current density and potential as a function of velocity at different pH.

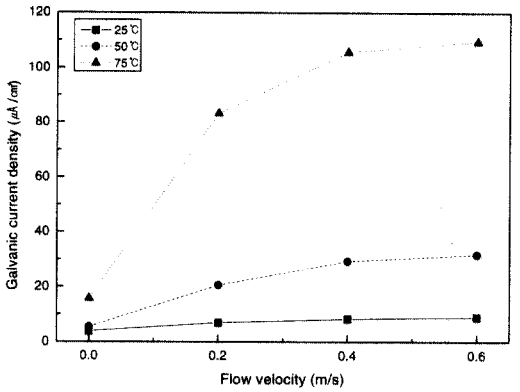

(a) Current density

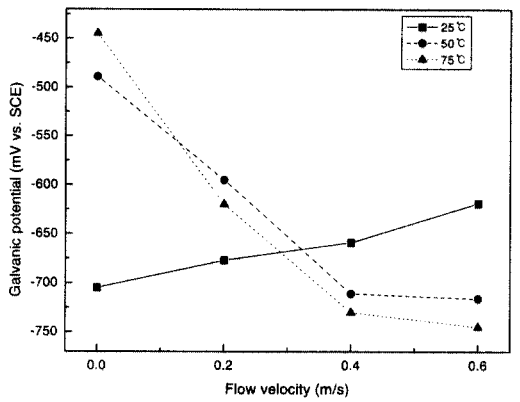

(b) Potential

Fig. 7. Galvanic current density and potential as a function of velocity at different temperature

3.3 Effect of temperature

Figure 7 exhibits the galvanic current density and galvanic potential as a function of velocity at different temperature. This showed that the current density largely increased as temperature increased, but the galvanic potential decreased with increasing velocity at 50℃ and 75℃.

Bignold[16] showed that the open-circuit potential of CS is lowered during dissolution of magnetite(FAC). Increased flow velocities, which lead to increased FAC rates, lead to lower open-circuit potentials, with the size of the shift being dependent on the pre-existing metal-loss rate. Since the growth of magnetite involves diffusion of ions through the oxide into the solution, an increase in flow velocity will increase their rate of removal due to the decrease in boundary layer thickness. The increase in temperature increases the solubility of the magnetite which results in a dissolution of the film as a result of the reaction.

$$Fe_3O_4 + 2(OH^-) = 2FeOOH + FeO_2^{2-}$$

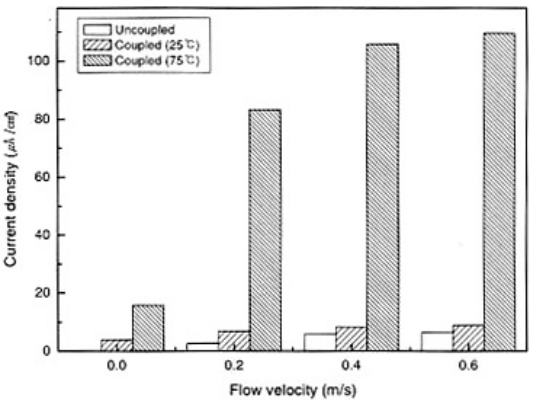

Fig. 8. Corrosion current density of carbon steel as a function of velocity, temperature and galvanic coupling.

Therefore the behavior of the corrosion in elevated temperature condition will depend upon whether the rate of film formation or the rate of film dissolution is predominant.[17] Thus, the continuous increment of current and decay of potential at 50℃ and 75℃ show that the process of film dissolution is dominant under these conditions. Consequently, the much larger effect of flow velocity at 75℃ may be due to an increase in solubility of magnetite with increase in temperature from 25℃ to 75℃, which accelerated the galvanic corrosion between CS and SS.

Figure 8 shows the corrosion current density of CS as a function of velocity and temperature at uncoupled and coupled condition. This indicated that the corrosion of CS(anode) increased by coupling with SS(cathode). Particularly, the corrosion current density increased about 10 orders of magnitude with increased in temperature from 25℃ to 75℃ at all velocities.

As a result, there was a little increase on corrosion current density at room temperature by galvanic coupling and fluid flowing, because the galvanic corrosion process was controlled by cathodic reaction. However, increment of temperature and velocity creates dramatic increase in FAC rate by the dissolution of magnetite.

3.4 Surface observation

Figure 9 shows the scanning electron micrographs of corroded surfaces after the galvanic corrosion tests. For a stationary condition, the surface was covered by uniform oxide, which

However, when a presence of fluid flow, the oxide was locally removed from the surface and corrosion attack was accelerated by galvanic effect.

XRD peaks of CS obtained from rusting surfaces after galvanic corrosion test in alkaline-chloride solutions are given in Figure 10. The rust layers formed at pH 8 and 9 are mainly composed of magnetite(Fe_3O_4). At pH 10,

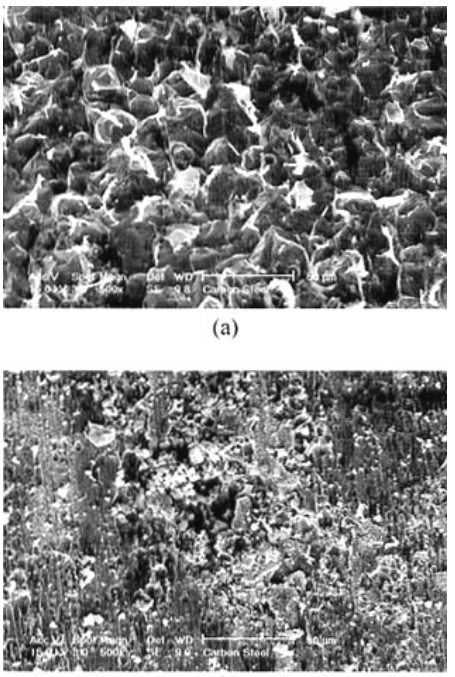

Fig. 9. SEM micrographs of CS after galvanic corrosion test: (a) 0 m/s, (b) 0.2 m/s

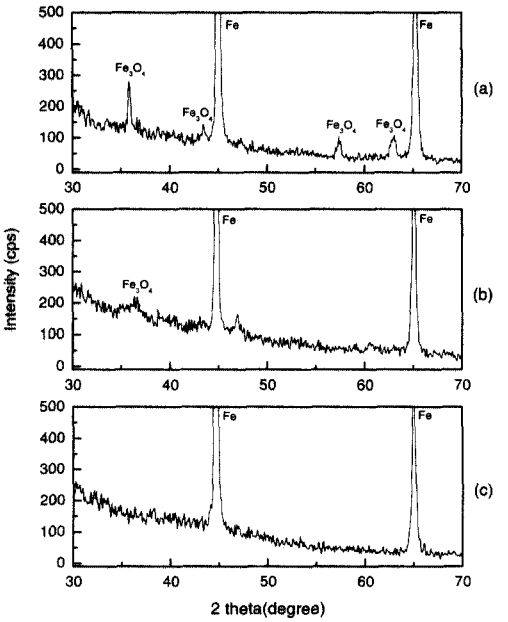

Fig. 10. XRD analysis results of CS after galvanic corrosion test:(a) pH 8, (b) pH 9, (c) pH 10

however, corrosion product was not detected due to a slight attack.

Figure 11 shows the scanning electron micrographs of cross-section as a function of temperature after the galvanic corrosion tests. The rust layer formed at room temperature exhibited a uniform, adherent and continuous structure. In contrast, the rust layer formed at 75℃ was not a uniform and continuous structure. The reduced galvanic corrosion resistance of the CS was attributed by the dissolution of magnetite due to the presence of fluid flow and the elevation of temperature.

4. Conclusions

1) CS showed active corrosion behavior, whereas SS exhibited passive behavior in alkaline-chloride solutions.

2) The corrosion potential of CS and SS increased with increasing flow velocity. Increasing flow velocity for the CS caused the corrosion rate to increase due to an increase in the cathodic reaction rate. While in the case of SS, increasing flow rates shifted the passive current density in the noble direction, indicating increased stability of the passive film.

3) The galvanic corrosion between CS and SS was accelerated as the presences of corrosion product and fluid flow. This was controlled by the increment of anodic or cathodic reaction rates at room temperature.

4) The galvanic corrosion rate reduced as increasing pH, caused by formation of stable oxide.

5) The rust layer formed on the CS in a deaerated alkaline-chloride solution was mainly composed of magnetite (Fe_3O_4). Due to the increased dissolution rate of the

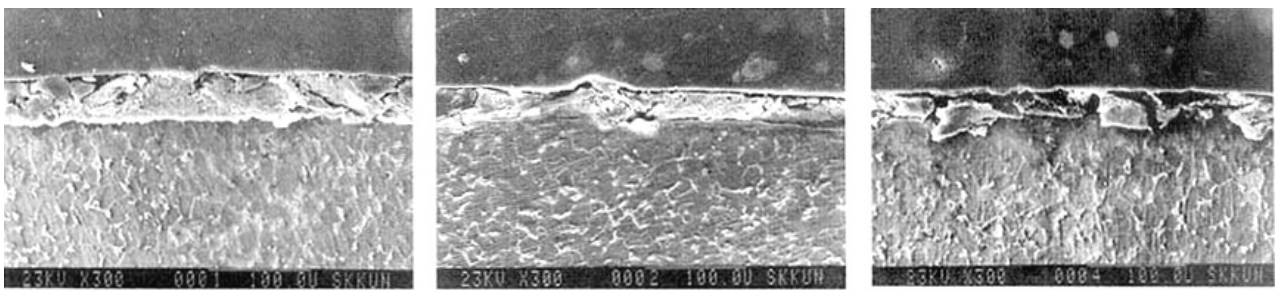

(a) (b) (c)

Fig. 11. SEM micrographs after galvanic corrosion test; (a) 25℃, (b) 50℃, (c) 75℃

magnetite, the galvanic corrosion rates can be very high in the fluid flowing high temperature environment.

References

1. D. A. Jones, in Principles and Prevention of Corrosion, Prentice Hall, NJ, USA, 2 (1996).
2. J. Perkins, K. J. Graham, G. A. STORM, G. Leumer and R. P. Schack, *Corrosion*, **35**, 23 (1979).
3. H. M. Shalaby, S. Attari, W. T. Riad, and V. K. Gouda, *Corrosion*, **48**, 206 (1992).
4. T. M. Laronge and M. A. Ward, in *CORROSION/99*, NACE, 345 (1999).
5. Flow-Accelerated Corrosion in Power Plants, EPRI, Preasant Hill, CA: EPRI-TR-10661, 3 (1996).
6. F. Mansfeld and J. V. Kenkel, in *Galvanic and Pitting Corrosion-Field and Laboratory Studies*, ASTM STP 576, ASTM, Philadelphia, 20 (1976).
7. D. C. Silverman, *Corrosion*, **44**, 42 (1988).
8. R. A. Holser, G. Prentice, R. B. Pond Jr., and R. Guanti, *Corrosion*, **46**, 764 (1990).
9. D. R. Gabe, *J. of App. Electrochem.*, **4**, 91 (1974).
10. H. P. Hack, in *Galvanic CorrosionTtest Methods*, NACE, Houston, 15 (1993).
11. F. Mansfeld, *Corrosion*, **32**, 380 (1976).
12. F. Mansfeld and J.V. Kenkel : *Corrosion*, **33**, 236 (1977).
13. B. E. Brown, H. H. Lu and D. J. Duquette, *Corrosion*, **48**, 970 (1992).
14. H. H. Uhlig and R. W. Revie, in Corrosion and Corrosion Control, John Wiley, USA, 71 (1985).
15. M. Pourbaix, in Atlas of Electrochemical Equilibria, NACE, Houston, 312 (1974).
16. G. J. Bignold, *Water Chemistry*, **3**, 219 (1983).
17. S. Giddey, B. Cherry, F. Lawson, and M. Forsyth, *Corrosion Science*, **40**, 839 (1998).